**References and Notes**

1. G. P. Smith, *Science* **228**, 1315 (1985); S. Cwirla, E. A. Peters, R. W. Barrett, W. J. Dower, *Proc. Natl. Acad. Sci. U.S.A.* **87**, 6378 (1990); J. K. Scott and G. P. Smith, *Science* **249**, 386 (1990); J. J. Devlin, L. C. Panganiban, P. E. Devlin, *ibid.*, p. 404.
2. P. Colas *et al.*, *Nature* **380**, 548 (1996).
3. G. Caponigro *et al.*, *Proc. Natl. Acad. Sci. U.S.A.* **95**, 7508 (1998).
4. K. T. O'Neil *et al.*, *Proteins Struct. Funct. Genet.* **14**, 509 (1992).
5. E. H. Serpersu, D. Shortle, A. S. Mildvan, *Biochemistry* **26**, 1289 (1987).
6. F. A. Cotton, E. E. Hazen Jr., M. J. Legg, *Proc. Natl. Acad. Sci. U.S.A.* **76**, 2551 (1979).
7. The library in *Escherichia coli* contained $1.7 \times 10^8$ members, of which more than $1.14 \times 10^8$ directed the synthesis of peptamers. The synthetic staphylococcal nuclease gene was assembled in two cloning steps: 15 oligonucleotides were annealed and ligated to form double-stranded $NH_2$-terminal (177 bases) and COOH-terminal (330 bases) fragments that were ligated separately to vector (pTCN13) cut with Bst EII and Eco RI and with Eco RI and Sal I, respectively. The Eco RI and Sal I sites allow insertion of a loop that replaces amino acids 19 to 27 of the mature staphylococcal nuclease. The resulting constructs were digested with Eco RI and Xba I and ligation of the staphylococcal nuclease gene-containing fragments assembled the full ORF fused to a hemagglutinin epitope tag at the $NH_2$-terminus and to a stretch of six histidine residues (pTCN22) at the COOH-terminus. The random peptide insert was prepared by self-annealing the following oligonucleotide: 5′-CCC-GAATTCTTCGGTGGT$(NNS)_{16}$GGTGGTGTCGACAC-3′ [N = A:T:G:C (1:1:1:1), S = G:C (1:1)]. Annealed DNA was extended by using the Klenow fragment of DNA polymerase I, and the double-stranded product was cut with Eco RI and Sal I to create two equivalents of library DNA that were ligated to the staphylococcal nuclease construct (pTCN22) cut with Eco RI and Sal I, installing library DNA in-frame.
8. The expression vector pTCN23 carried the replicator of the 2-μm circle, an endogenous yeast high-copy plasmid, the *PGK1* promoter [A. Chambers, C. Stanway, A. J. Kingsman, S. M. Kingsman, *Nucleic Acids Res.* **16**, 8245 (1988)], and had codon usage optimized according to Sharp and Li [P. M. Sharp and W. H. Li, *Nucleic Acids Res.* **15**, 1281 (1987).
9. K. G. Hardwick, *Trends Genet.* **14**, 1 (1998).
10. I. Herskowitz, *Cell* **80**, 187 (1995).
11. X. Li and R. B. Nicklas, *Nature* **373**, 630 (1995); C. L. Rieder, R. W. Cole, A. Khodjakov, G. Sluder, *J. Cell Biol.* **130**, 941 (1995); W. A. Wells and A. W. Murray, *ibid.* **133**, 75 (1996).
12. D. P. Cahill, *et al.*, *Nature* **392**, 300 (1998).
13. M. A. Hoyt, L. Totis, B. T. Roberts, *Cell* **66**, 507 (1991); R. Li and A. W. Murray, *ibid.*, p. 519 (1991).
14. K. G. Hardwick, E. Weiss, F. C. Luca, M. Winey, A. W. Murray, *Science* **273**, 953 (1996).
15. Unless otherwise indicated, all experiments in this study were done in strains isogenic to W303. A single selection strain, DA2050A (*a/a bar1/bar1 mec1-1/mec1-1 CDC28VF::LEU2/CDC28-VF::LEU2 GAL1-MPS1/GAL1-MPS1*), was engineered to identify inhibitors of the spindle checkpoint or of the pheromone response pathway. The *bar1* mutation increases sensitivity to α factor by removing a protease that degrades the pheromone, and the *CDC28-VF* mutation blocks the ability of cells to adapt to overexpression of Mps1 from the *GAL1* promoter. The *mec1-1* mutation, which abolishes the DNA damage checkpoint, is irrelevant to the experiments reported here.
16. For both selections, transformants were grown on uracil-deficient plates for 2 days. Cells were scraped from these plates, and aliquots were plated onto selection plates [lacking uracil and containing galactose (−uracil/+galactose) for the spindle checkpoint selection; lacking uracil and containing α factor (−uracil/+α factor) (1 μg/ml) for the pheromone pathway selection] and grown at 30°C for 2 or 3 days. Plasmid DNA was recovered from the entire population of colonies that grew on these plates, purified, amplified by transformation into *E. coli*, and retransformed into DA2050A to enrich for peptamers that conferred resistance as opposed to genomic mutations that caused resistance. Cell populations harboring active peptamers typically grew as lawns on selection plates, and individual plasmids were isolated from these plates and retested to confirm that they gave plasmid-dependent resistance.
17. T. C. Norman and A. W. Murray, unpublished data.
18. S. Fields and O. Song, *Nature* **340**, 245 (1989).
19. F. A. Barr, M. Puype, J. Vandekerckhove, G. Warren, *Cell* **91**, 253 (1997).
20. A. J. Lustig, *Curr. Opin. Genet. Dev.* **8**, 233 (1998).
21. M. S. Singer *et al.*, *Genetics* **150**, 613 (1998).
22. Y. Cao, B. R. Cairns, R. D. Kornberg, B. C. Laurent, *Mol. Cell. Biol.* **17**, 3323 (1997).
23. K. Tedford, S. Kim, D. Sa, K. Stevens, M. Tyers, *Curr. Biol.* **7**, 228 (1997).
24. H. D. Madhani and G. R. Fink, *Science* **275**, 1314 (1997).
25. T. C. Norman, S. M. O'Rourke, A. W. Murray, unpublished results.
26. S. Henchoz *et al.*, *Genes Dev.* **11**, 3046 (1997).
27. B. J. Stevenson, N. Rhodes, B. Errede, G. F. Sprague Jr., *Genes Dev.* **6**, 1293 (1992).
28. S. M. O'Rourke and I. Herskowitz, *ibid.* **12**, 2874 (1998).
29. F. Posas, E. A. Witten, H. Saito, *Mol. Cell. Biol.* **18**, 5788 (1998).
30. M. R. Rad, G. Xu, C. P. Hollenberg, *Mol. Gen. Genet.* **236**, 145 (1992).
31. Abbreviations for the amino acid residues are as follows: A, Ala; C, Cys; D, Asp; E, Glu; F, Phe; G, Gly; H, His; I, Ile; K, Lys; L, Leu; M, Met; N, Asn; P, Pro; Q, Gln; R, Arg; S, Ser; T, Thr; V, Val; W, Trp; and Y, Tyr.
32. A yeast ORF-Gal4 activation domain fusion array has been assembled that expresses about 85 to 90% of the predicted ORFs of *S. cerevisiae* in strain pJ69-4a [P. James, J. Halladay, E. Craig *Genetics* **144**, 1425 (1996)]. In this strain, *GAL4* is absent and the reporters *HIS3* and *ADE2* are under Gal4 control. To probe the Gal4-AD fusion array for protein-protein interactions, we mated the array to a strain expressing a Gal-4–DNA binding domain fusion. After selecting for diploids, we identified two-hybrid positives by testing diploids on plates containing different concentrations of 3-aminotriazole.
33. L. H. Hwang *et al.*, *Science* **279**, 1041 (1998).
34. J. L. DeRisi, V. R. Iyer, P. O. Brown, *ibid.* **278**, 680 (1997).
35. We performed the following competitive hybridizations: wild-type cells with or without peptamer S-1, with or without peptamer S-5, and with or without expression of $SIR4^{DN}$. Each comparison was done on four arrays composed of two pair of hybridizations done with reversal of the fluorophore labelings to eliminate biases of fluorophore incorporation. We used two different sources of mRNAs for labeled cDNA production, including a total RNA protocol (http://www.nhgri.nih.gov/DIR/LCG/15K/HTML/) and twice-purified polyadenylated mRNAs [(M. J. Marton *et al. Nature Med.* **4**, 1293 (1998)].


36. Supported by grants from NIH, Human Frontier Science Program, and Chiron (A.W.M.); an NIH senior fellowship (T.C.N.); an NIH grant and the Herbert W. Boyer Fund (S.M.O.); and NIH grant P41-RR11823 (B.L.D. and S.F.). S.F. is an Investigator of the Howard Hughes Medical Institute. We thank L. Hartwell, I. Herskowitz, L. Huang, and J. Rine for yeast strains and plasmids; T. Geyer, Alejandro Colman-Lerner, and R. Brent for communicating unpublished results; and D. Gottschling, I. Herskowitz, L. Pillus, J. Simon, and members of the Seattle Project and the Murray laboratory for valuable discussions.

20 April 1999; accepted 16 June 1999


# Neuronal Protection in Stroke by an sLe$^x$-Glycosylated Complement Inhibitory Protein


**Judy Huang,[1] Louis J. Kim,[1] Richard Mealey,[2] Henry C. Marsh Jr.,[2] Yuan Zhang,[1] Andrea J. Tenner,[3] E. Sander Connolly Jr.,[1] David J. Pinsky[1]***



**Glycoprotein adhesion receptors such as selectins contribute to tissue injury in stroke. Ischemic neurons strongly expressed C1q, which may target them for complement-mediated attack or C1qRp-mediated clearance. A hybrid molecule was used to simultaneously inhibit both complement activation and selectin-mediated adhesion. The extracellular domain of soluble complement receptor–1 (sCR1) was sialyl Lewis x glycosylated (sCR1sLe$^x$) to inhibit complement activation and endothelial-platelet-leukocyte interactions. sCR1 and sCR1sLe$^x$ colocalized to ischemic cerebral microvessels and C1q-expressing neurons, inhibited neutrophil and platelet accumulation, and reduced cerebral infarct volumes. Additional benefit was conferred by sialyl Lewis x glycosylation of the unmodified parent sCR1 molecule.**


Interrupting blood flow to the brain, even for relatively short periods, can trigger inflammatory events within the cerebral microvasculature that can exacerbate cerebral tissue injury. The tissue damage that accrues is amplified by activation of both inflammatory and coagulation cascades within postischemic cerebral microvessels, impairing recovery of blood flow and causing collateral damage to bystander neurons. In a murine model of stroke, increased expression of the glycoprotein adhesion receptors P-selectin (*1*) and ICAM-1 (*2*) promotes leukocyte recruitment. Mice lacking these adhesion receptors exhibit


[1]Columbia University, College of Physicians and Surgeons, 630 West 168th Street, New York, NY 10032, USA. [2]Avant Immunotherapeutics, Inc., 119 Fourth Avenue, Needham, MA 02494, USA. [3]University of California, Department of Molecular Biology and Biochemistry, Irvine, CA 92697, USA.

*To whom correspondence should be addressed. E-mail: djp5@columbia.edu

reduced leukocyte recruitment and improved postischemic perfusion and are moderately protected from cerebral injury in stroke. Microvascular thrombosis, which occurs in situ in cerebral microvessels downstream from the site of primary occlusion, can be inhibited by the blockade of platelet glycoprotein IIb/IIIa receptor (*3*).

Although neuronal blood supply may be diminished by microvascular thrombosis and leukostasis, and neurons may be damaged by their proximity to inflammatory foci, it is also possible that inflammatory mechanisms may subject neurons to direct attack. Although neurons do not normally express complement proteins, in Alzheimer's disease, neurons synthesize and express C1q (*4*), a critical initiator of the classical pathway of complement activation and a ligand for C1qRp, a receptor on myeloid cells (including microglia) that enhances phagocytosis (*5*). A role for complement activation in stroke has not been elucidated, though it has been shown to play a role in ischemia-induced damage in other tissues (*6, 7*).

Brain tissue sections obtained from mice subjected to 45 min of middle cerebral artery (MCA) occlusion followed by 23 hours of reperfusion showed prominent neuronal staining for C1q in the ipsilateral cerebral cortex (Fig. 1A). Neurons in the contralateral cerebral cortex expressed C1q at barely detectable levels (Fig. 1B), and neurons from nonischemic control brain did not express any detectable C1q (Fig. 1D). As a specificity control for these experiments, murine C1q was purified (*8*) and then mixed with the primary antibody to C1q (anti-C1q) before staining. These experiments confirmed a specific increase in C1q expression in neurons in the ischemic cerebral cortex but not in the nonischemic cerebral cortex (Fig. 2A). Protein immunoblot analysis demonstrated increased density of a band that was immunoreactive for murine C1q in ipsilateral but not contralateral hemispheric tissue extracts 24 hours after stroke (amounts of C1q protein in nonischemic tissue were similar to that observed in nonischemic control brain). Not only was this band immunoreactive for C1q, but it comigrated with a purified C1q-positive control at the expected relative molecular mass of ~28 kD (Fig. 2B).

To examine the functional effects of complement activation in the context of ischemia-reperfusion–driven expression of neuronal C1q, we studied the effects of a potent inhibitor of complement activation, soluble complement receptor–1 (sCR1) (*7*). In nonstroke (control) brain, an affinity-purified antibody to human sCR1 failed to stain any structures (Fig. 1C). However, we used this same antibody to localize sites of sCR1 binding in stroke. When sCR1 was infused into mice just before stroke and brain tissue was then studied after reperfusion, sCR1 was found to colocalize to neurons that express C1q (Fig. 1, E and F, arrowheads), as well as intraluminally in the cerebral microvessels where C1q was not expressed (Fig. 1, E and F, arrows). Both neuronal bodies and their axonal processes in the ischemic region bound sCR1 (Fig. 1G). In contrast, neurons examined in the contralateral cortex from the same mouse bound little if any sCR1 (Fig. 1H).

Infusion of sCR1 into mice immediately before stroke caused a modest reduction in cerebral tissue injury (*9*) (Fig. 3, A and B). However, because leukocyte adhesion receptor expression (*1, 2*) and thrombosis (*3*) in the postischemic cerebral microvasculature may occur independent of complement activation yet still contribute to cerebral tissue injury in stroke, we sought to modify sCR1 to inhibit these additional deleterious inflammatory and thrombotic events. Because selectin expression is up-regulated in stroke (*1, 10*), we hypothesized that a single molecule that inhibits both complement activation and selectin-mediated adhesive events might simultaneously limit both inflammatory and coagulant reactions in stroke. We therefore covalently modified sCR1 by sialyl Lewis x ($sLe^x$) glycosylation (*11*). We expressed sCR1 in CHO LEC11 cells, which are capable of incorporating the $sLe^x$ tetrasaccharide in the posttranslational glycosylation of

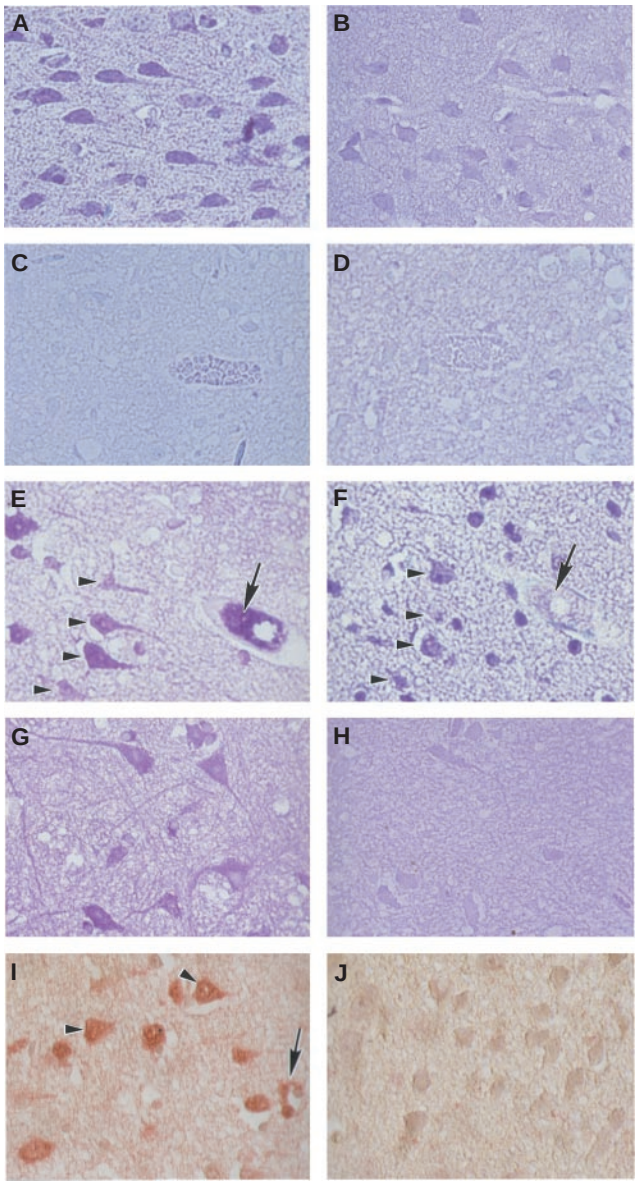


**Fig. 1.** Ischemia-driven neuronal C1q expression, and localization of sites of sCR1 and sCR1$sLe^x$ binding. Adjacent tissue sections were incubated with either a primary rabbit antibody to mouse C1q [62 μg/ml, 1:150 dilution in phosphate-buffered saline (PBS); this antibody is a purified immunoglobulin G (IgG) with murine C1q as the rabbit immunogen], or with rabbit affinity-purified anti-sCR1 (*19*) (42 μg/ml, 1:50 dilution in PBS) at 37°C for 60 min. (**A** and **B**) Sections of brain from a control mouse subjected to 45 min of cerebral ischemia and 23 hours of reperfusion. Immunostaining with anti-C1q demonstrates immunoreactivity on neuronal surfaces in the ipsilateral (A) cerebral cortex, with minimal staining in the contralateral (nonischemic) cortex (B). (**C** and **D**) Section of brain from an untreated (nonoperated) mouse. Neither sCR1 (C) nor C1q (D) immunoreactivity can be detected. (**E** and **F**) Adjacent brain sections from the ipsilateral hemisphere of an sCR1-treated mouse that underwent stroke immunostained with either anti-sCR1 (E) or anti-C1q (F). Arrowheads indicate neurons that exhibit immunoreactivity for both sCR1 and C1q in adjacent sections. Arrows point to a cerebral microvessel, which stains intraluminally for sCR1 but not C1q. (**G** and **H**) Ipsilateral and contralateral brain sections of an sCR1-treated mouse that underwent stroke. The ipsilateral section (G) demonstrates detailing of neuronal bodies and axonal processes from immunoreactivity to anti-sCR1. The contralateral section (H) taken from the same mouse shows minimal immunoreactivity for sCR1. (**I** and **J**) Ipsilateral sections of a brain from an sCR1$sLe^x$-treated mouse that underwent stroke. Neuronal immunoreactivity for sCR1 is shown (arrowheads) in the ipsilateral cerebral cortex (I), as well as some immunoreactivity within a cerebral microvessel (arrow). Contralateral cerebral cortex from the same mouse (J) shows minimal immunoreactivity for sCR1.

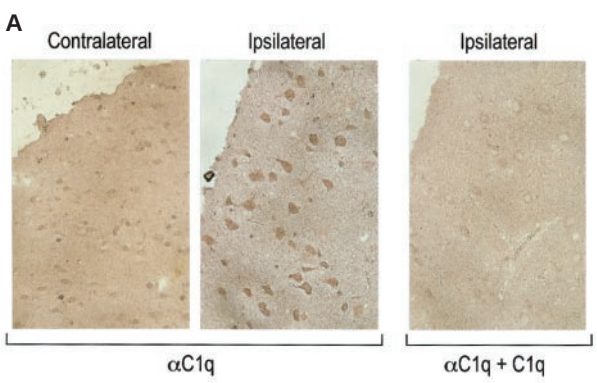


**Fig. 2.** Effect of cerebral ischemia on neuronal C1q expression. (**A**) The minimum concentration of IgG that gave positive immunostaining was determined (1:400 dilution), then mixing experiments were performed with an excess of purified murine C1q to block the primary antibody to demonstrate specificity of the neuronal immunostaining. The contralateral (nonischemic) region did not stain with primary antibody alone (23 μg/ml; 1:400 dilution), although the ipsilateral (ischemic) region exhibited neuronal immunoreactivity under the identical staining conditions. When antigen (120 μg/ml, ~fivefold excess) was mixed with the primary antibody (overnight incubation at 4°C) before experiments, ipsilateral staining was completely blocked. Similarly, no positive immunostaining was detected in the contralateral region in this blocking experiment (not shown). (**B**) Protein immunoblot analysis for murine C1q. (Reducing conditions were used, 12% SDS-PAGE, 140 μg of total protein per lane, and a dilution of primary antibody of 1:1000). Sites of primary antibody binding were detected with a donkey horseradish-peroxidase–conjugated secondary anti–rabbit IgG (1:2000) and the enhanced chemiluminescent method of immunodetection. Purified murine C1q (250 ng) was used as a positive control (*8*). Tissue samples from two normal, untreated mice (lanes marked control brain) showed only slight immunoreactivity, similar to that seen in the contralateral hemispheric extracts from two separate mice (mouse A and mouse B) taken 24 hours after stroke. In contrast, a strongly immunoreactive band was seen for both ipsilateral (ischemic) hemispheres from these same mice.

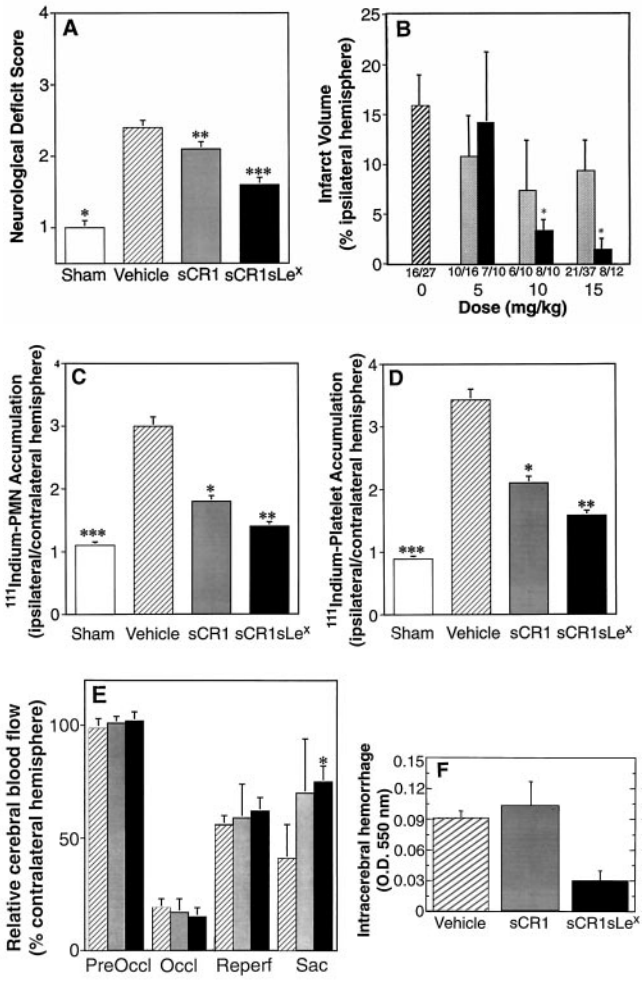


**Fig. 3.** Effect of sCR1 or sCR1sLe$^x$ administration on outcomes after stroke. For the surgical procedure, neurological scoring, and infarct volume analysis, operators were blinded to the treatment regimen. (**A**) Compared with sham-operated animals ($n = 10$), neurological deficit was greater after middle cerebral arterial occlusion and reperfusion in vehicle-treated animals ($n = 27$, * = $P <$ 0.005). Neurological deficit was less in sCR1-treated (15 mg/kg, $n = 37$) and sCR1sLe$^x$-treated (15 mg/kg, $n = 12$) animals compared with vehicle-treated controls; ** = $P < 0.05$, and *** = $P < 0.05$, respectively). (**B**) Infarct volumes were determined by staining serial cerebral sections with triphenyl tetrazolium chloride (TTC) and performing computer-based planimetry of the negatively (infarcted) staining areas to calculate infarct volume (with National Institutes of Health image software). Infarct volumes, with dose-response relation of sCR1 and sCR1sLe$^x$ [$n = 27$ for vehicle-treated animals (0 mg/kg) (striped bar)]; $n =$ 16, 10, and 37 for sCR1 (gray bars) and $n = 10$, 10, and 12 for sCR1sLe$^x$ (black bars), for the 5, 10, and 15 mg/kg doses respectively. Significantly lower infarct volumes were observed in 10 mg/kg and 15 mg/kg doses of sCR1sLe$^x$ relative to vehicle (* = $P < 0.05$). Survival figures are indicated below each bar as the number of animals surviving until they were killed at 24 hours (numerator) over the total number of experiments performed (denominator). Panels (C to F) illustrate the effect of preoperative sCR1 (15 mg/kg) or sCR1sLe$^x$ (15 mg/kg) administration on neutrophil accumulation, platelet accumulation, relative cerebral blood flow, and intracerebral hemorrhage 24 hours after stroke in mice. (**C**) $^{111}$In-labeled PMNs administered preoperatively demonstrate progressively decreasing accumulation in the ipsilateral versus contralateral hemisphere in sCR1- and sCR1sLe$^x$-treated animals compared with vehicle treated controls (* = $P < 0.03$; ** = $P < 0.003$; *** = $P < 0.0001$). Ten mice were used to obtain pooled PMNs; $n = 8$, 7, 5, and 6 for sham, vehicle, sCR1, and sCR1sLe$^x$, respectively. Neutrophil accumulation after focal cerebral ischemia and reperfusion was determined by preoperative injection of $1.5 \times 10^5$ $^{111}$In-labeled PMNs administered intravenously immediately before surgery. Brain harvest was performed 24 hours after middle cerebral artery occlusion, and the determination of the differential extent of neutrophil accumulation in the affected ipsilateral hemisphere was calculated as ipsilateral/contralateral counts per million (cpm). (**D**) Platelet accumulation studies with $^{111}$In-labeled platelets demonstrate no difference in accumulation in ipsilateral versus contralateral hemispheres in sham mice. sCR1- and sCR1sLe$^x$-treated mice show progressively diminished rates of platelet accumulation compared with vehicle-treated controls (* = $P < 0.05$; ** = $P < 0.005$; *** = $P < 0.0002$ versus vehicle-treated controls). Ten mice were used to obtain pooled platelets; $n = 6$, 6, 5, and 4 for sham, vehicle, sCR1, and sCR1sLe$^x$, respectively. Platelet accumulation was determined with $^{111}$In-labeled platelets, collected and prepared as previously described (*3*). Mice received an intravenous injection of $5.0 \times 10^6$ $^{111}$In-labeled platelets immediately before surgery. Brains were harvested at 24 hours after middle cerebral artery occlusion, and deposition in the affected cerebral hemisphere was determined by the calculation of ipsilateral/contralateral counts per minute (cpm). (**E**) Relative cerebral blood flow was measured at baseline (PreOccl), immediately after middle cerebral artery occlusion (Occl), 45 min later immediately after withdrawal of the occluding suture (Reperf), and immediately before sacrifice at 24 hours (Sac) [$n = 7$, 12, and 9 for vehicle (striped bars), sCR1 (gray bars), and sCR1sLex (black bars), respectively; * = $P <$ 0.05 versus vehicle]. We obtained measurements of relative cerebral blood flow as previously described (*1–3, 14*) using a straight laser Doppler flow probe placed 2 mm posterior to the bregma, and 6 mm to each side of midline using a stereotactic micromanipulator, keeping the angle of the probe perpendicular to the cortical surface. These cerebral blood flow measurements, expressed as the ratio of ipsilateral to contralateral blood flow, were obtained at baseline, immediately after withdrawal of the occluding suture, and before sacrifice at 24 hours. (**F**) Mice were treated with vehicle, sCR1 (15 mg/kg), or sCR1sLe$^x$ (15 mg/kg) immediately before surgery, and intracerebral hemorrhage measured at 24 hours with a spectrophotometric assay that has been validated for use in mice with stroke (*20*). The means ± SEM of five animals are shown. $P$ = not significant for all comparisons.

proteins. This glycoprotein product, sCR1sLe$^x$, includes at least 10 sLe$^x$ moieties per sCR1 molecule (*11*). In vitro experiments demonstrated that sCR1sLe$^x$, but not sCR1, binds cell surface E-selectin and also blocks P-selectin–mediated cellular adhesion (*11*).

sCR1sLe$^x$ given before stroke could be detected bound to neurons and within vascular lumina 24 hours after stroke (Fig. 1, I and J). In its ability to minimize the volume of infarcted cerebral tissue and reduce neurological deficit, sCR1sLe$^x$ was more potent than sCR1 (Fig. 3, A and B). Mice treated with sCR1 before middle cerebral artery occlusion demonstrated less neurological deficit at 24 hours than vehicle-treated controls (Fig. 3A). sCR1sLe$^x$ treatment diminished neurological impairment even further. Mean infarct volumes were lower in the sCR1-treated animals, although large standard errors precluded ascribing statistical significance to these values. However, sCR1sLe$^x$ markedly diminished infarct volume in a dose-dependent fashion, with up to an 11-fold reduction in cerebral infarct volume observed at the highest dose tested (15 mg per kilogram of body weight) (Fig. 3B) (*12*).

Because sCR1 and sCR1sLe$^x$ localize not only to C1q-expressing neurons but to ischemic cerebral microvessels, we examined vascular mechanisms by which these compounds may confer protection to cerebral tissue in stroke. We administered $^{111}$In-labeled neutrophils immediately before surgery and then quantified their accumulation in ischemic cerebral tissue. Compared with animals undergoing sham surgery, animals subjected to middle cerebral artery occlusion and reperfusion exhibited a nearly threefold increase in ipsilateral leukocyte accumulation (Fig. 3C). Pretreatment with sCR1 (15 mg/kg) caused a 1.7-fold reduction in leukocyte accumulation. However, sCR1 treatment did not reduce neutrophil accumulation to baseline, implicating additional noncomplement-dependent mechanisms of leukocyte recruitment in stroke. sCR1sLe$^x$ further reduced polymorphonuclear leukocyte accumulation in the ipsilateral cerebral cortex, to a level just slightly above baseline.

When the accumulation of $^{111}$In-labeled platelets was similarly tracked, sCR1sLe$^x$ caused even greater inhibition of platelet accumulation than sCR1 alone (Fig. 3D). These data support the observation that leukocytes and platelets demonstrate substantial adhesion-receptor-dependent interactions (*13*), which may amplify microvascular thrombosis. Postischemic cerebral hypoperfusion, which is dependent upon the severity of the cerebral ischemic insult and which may be caused by microvascular thrombosis, leukocyte capillary plugging, vascular damage, or abnormal vasoreactivity (*1–3, 14, 15*), is also a feature of the stroke model used in these studies. Laser Doppler measurements showed equivalent blood flows between ipsilateral and contralateral cerebral cortices at baseline, upon occlusion of the middle cerebral artery, and immediately upon withdrawal of the occluding suture (Fig. 3E). However, by the time the mice were killed, ipsilateral blood flow was significantly higher in sCR1sLe$^x$-treated animals, and at an intermediate level in the sCR1-treated animals. The failure of blood flow to return completely back to baseline suggests the recruitment of additional effector mechanisms beyond those that can be inhibited by complement and selectin blockade. Because of concerns that an antiselectin agent, which inhibits platelet recruitment, may increase intracerebral hemorrhage, we performed experiments to examine this possibility. We saw no increase in intracerebral hemorrhage after therapy; there was even a trend toward a decrease with the antiselectin agent (Fig. 3F). Other physiological variables examined did not suggest that the tested compounds had any other adverse effects in mice (*16*). Even after longer observation periods (72 hours), the beneficial effects of sCR1sLe$^x$ administration were sustained (Fig. 4A).

In clinical stroke, patients present after the onset of the ischemic event. Any therapeutic intervention must therefore be effective after the onset of ischemia. Both compounds (15 mg/kg) were administered 45 min after ischemic onset immediately after removal of the occlusion. sCR1sLe$^x$ maintained cerebroprotective efficacy, as reflected in diminished infarct volumes, albeit less than that seen during preischemic administration (Fig. 4B). Blockade of complement activation after the ischemic event with sCR1 was of intermediate efficacy between that of vehicle and that of sCR1sLe$^x$. Neurological function and relative cerebral blood flow at 23 hours of reperfusion were also improved by administration of sCR1sLe$^x$ after occlusion. For control versus sCR1sLe$^x$-treated animals, respectively, the data were as follows: neurological deficit score $2.8 \pm 0.3$ versus $1.5 \pm 0.3$, $P < 0.02$; cerebral blood flow of the ipsilateral hemisphere relative to that of the contralateral hemisphere was $41 \pm 15\%$ versus $75 \pm 7\%$, $P < 0.05$. Although administration 45 min after ischemia in mice cannot be directly translated into clinical relevance without corroborative human data, a recent clinical trial showed that the average time from stroke onset to emergency room presentation was 57 min (although an additional 100 min were required for a CT scan before administration of tissue plasminogen activator) (*17*). If an "innocuous" agent can be given at presentation without the delay of an intervening CT scan, then an opportunity will open up for therapeutic intervention in stroke.

These studies demonstrate that ischemic neurons express C1q, presumably to flag the complement system to bring about their own demise or to aid in removing damaged cells, or both. It is not surprising that sCR1 targets and binds to C1q-expressing neurons, because CR1 has been shown to be a ligand for C1q (*18*). sCR1, a soluble, truncated form of the human complement receptor protein CR1, binds to proteins of the multisubunit C3 or C5 convertases formed as a result of complement activation to promote dissociation of the catalytic subunits (*7*). sCR1 is moderately cerebroprotective in the setting of reperfused stroke, reducing neutrophil and platelet recruitment. However, when this agent is glycosylated with sLe$^x$ to additionally inhibit selectin-mediated events, it significantly protects the reperfused brain against leukocyte and platelet recruitment and neuronal injury.

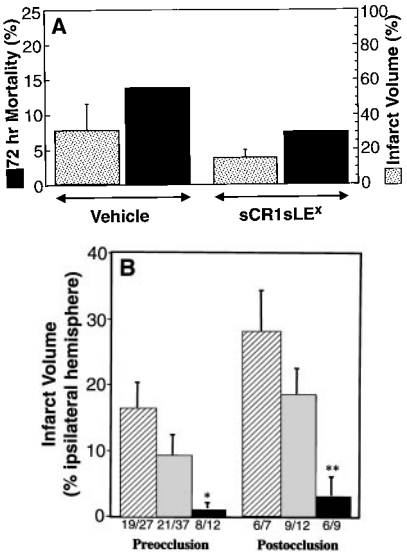


**Fig. 4.** Effect of complement/selectin blockade on delayed survival and effect of postischemic administration. (**A**) Effects of treatment on survival beyond 24 hours. sCR1sLe$^x$ (15 mg/kg, $n = 23$) or vehicle ($n = 22$) was administered immediately before surgery to a separate cohort of animals, and the delayed effects on cerebral infarct volumes and survival were recorded. By 72 hours, all mice that had not died beforehand were killed due to humane considerations (secondary to reduced oral intake and weight loss, and as mandated by our Institutional Animal Care and Use Committee-approved protocol). (**B**) Effect of postischemic administration of sCR1 or sCR1sLe$^x$ on cerebral infarction volumes. Compounds (15 mg/kg) or vehicle were administered 45 min after occlusion immediately after withdrawal of the middle cerebral arterial occluding suture. Preocclusion data are those shown in Fig. 2B (15 mg/kg dose data), repeated here for comparison to postischemic administration (* = $P < 0.03$ and ** = $P < 0.05$ versus vehicle); survival figures are indicated below each bar as the number of animals surviving until sacrifice at 24 hours (numerator) over the total number of experiments performed (denominator). Striped bars, vehicle; gray bars, sCR1; black bars, sCR1sLe$^x$.

**References and Notes**

1. E. S. Jr. Connolly *et al*., *Circ. Res.* **81**, 304 (1997).
2. E. S. Jr. Connolly *et al*., *J. Clin. Invest.* **97**, 209 (1996).
3. T. F. Choudhri *et al*., *ibid.* **102**, 1301 (1998).
4. A. Afagh, B. J. Cummings, D. H. Cribbs, C. W. Cotman, A. J. Tenner, *Exp. Neurol.* **138**, 22 (1996); S. A. Johnson *et al.*, *Neurobiol. Aging* **13**, 641 (1992).
5. A. R. Korotzer *et al*., *ibid.* **134**, 214 (1995).
6. Y. Naka, H. C. Marsh, S. M. Scesney, M. C. Oz, D. J. Pinsky, *Transplantation* **64**, 1248 (1997); M. Pemberton, G. Anderson, V. Vetvicka, D. E. Justus, G. D. Ross, *J. Immunol.* **150**, 5104 (1993); R. E. Chavez-Cartaya, G. P. DeSola, L. Wright, N. V. Jamieson, D. J. White, *Transplantation* **59**, 1047 (1995); J. Hill *et al*., *J. Immunol.* **149**, 1723 (1992).
7. H. F. Weisman *et al*., *Science* **249**, 146 (1990).
8. Murine C1q was purified from 50 ml of mouse sera (Sigma, St. Louis, MO) [F. Petry, K. B. M. Reid, M. Loos, *J. Immunol.* **147**, 3988 (1999)]. Briefly, the precipitate from dialysis of serum against 25 mM EGTA, pH 7.5, was resuspended in 0.5 M NaCl, 20 mM EDTA, pH 7.5, and loaded on a Superose 12 column. The positive fractions were then pooled, dialyzed against 20 mM EDTA, 20 mM Hepes, and the precipitate solubilized in SDS sample buffer and separated by SDS–polyacrylimide gel electrophoresis (SDS-PAGE). After staining with Coomassie blue to locate the bands, we excised the C1q bands and used them for immunization. The C1q antigen that was used for protein immunoblotting and for blocking experiments was purified by applying mouse serum (plus 10 mM EDTA) to a BioRex 70 column as described [A. J. Tenner, P. H. Lesavre, N. R. Cooper, *J. Immunol.* **127**, 648 (1981); K. R. Young, J. L. Ambrus Jr., A. Malbran, A. S. Fauci, A. J. Tenner, *ibid.* **146**, 3356 (1991)], followed by ammonium sulfate precipitation.
9. Before giving anesthesia to the mice, we examined them for neurological deficit 23 hours after reperfusion using a four-tiered grading system: 1, the animal demonstrated normal, spontaneous, movements; 2, the animal was noted to be turning toward the ipsilateral side; 3, the animal was observed to spin longitudinally (clockwise when viewed from the tail); and 4, the animal was unresponsive to noxious stimuli. This scoring system has been previously described for mice (*2*).
10. C. J. M. Frijns *et al*., *Stroke* **28**, 2214 (1997); Y. Okada *et al*., *ibid.* **25**, 202 (1994); H. P. Haring, E. L. Berg, N. Tsurushita, M. Tagaya, G. J. del Zoppo, *ibid.* **27**, 1386 (1996).
11. C. W. Rittershaus *et al*., *J. Biol. Chem.* **274**, 11237 (1999).
12. In an alternative way of measuring tissue injury in stroke, an indirect method of calculating infarct volumes was also used, based on the same TTC-stained serial cerebral sections [R. A. Swanson *et al*., *J. Cereb. Blood Flow Metab.* **10**, 290 (1990); T. N. Lin, Y. Y. He, G. Wu, M. Kahn, C. Y. Hsu, *Stroke* **24** 117 (1993)]. The effects of sCR1 and sCR1sLe$^x$ administration on infarction size persisted when the indirect method was used to perform the morphometric analysis of infarcted areas. Pretreatment with sCR1sLe$^x$ resulted in a significant reduction in infarct size from 11.4 ± 2.5% to 1.6 ± 0.9% ($P$ = 0.04), whereas pretreatment with sCR1 had only an intermediate effect on infarct size reduction to 7.4 ± 2.2% ($P$ = not significant). Furthermore, these effects were reproducible in cohorts that received either sCR1 or sCR1sLe$^x$ after the removal of the occluding suture. sCR1sLe$^x$ caused a decrease in infarct size from 16.6 ± 4.5% to 3.7 ± 1.2% ($P$ = 0.02), whereas sCR1 caused an intermediate reduction to 9.3 ± 2.7% ($P$ = not significant). All of the conclusions based on either method remain the same, but the values for the "indirect infarction volumes" are smaller than those for the "direct technique, as has been reported in previous comparisons of the two methods.
13. B. Furie and B. C. Furie, *Thromb. Haemostasis* **74**, 224 (1995); P. H. M. Kuijper *et al*., *Blood* **87**, 3271 (1996); T. G. Diacovo, S. J. Roth, J. M. Buccola, D. F. Bainton, T. A. Springer, *ibid.* **88**, 146 (1996).
14. J. Huang, L. J. Kim, A. Poisik, D. J. Pinsky, E. S. Connolly Jr., *Neurosurgery,* in press.
15. C. J. Prestigiacomo *et al*., *Stroke* **30**, 1110 (1999).
16. The administration of sCR1 has not previously been shown to have any adverse effects. In a rat model of hemorrhage and resuscitation, sCR1 had no adverse effects on arterial pressure, heart rate, or cardiac ouput [T. M. Fruchterman, D. A. Spain, M. A. Wilson, P. D. Harris, R. N. Garrison, *Surgery* **124**, 782 (1998)]. In pigs subjected to cardiopulmonary bypass with or without revascularization of ischemic myocardium, administration of sCR1 had no adverse effects on systemic or pulmonary hemodynamics [A. M. Gillinov *et al*., *Ann. Thorac. Surg.* **55**, 619 (1993); H. L. Lazar *et al*., *ibid.* **65**, 973 (1998)]. In our experiments, mice were subjected to administration of either sCR1 or sCR1sLe$^x$, followed by sternotomy and placement on a rodent ventilator (with room air) for direct sampling of left ventricular blood 3 hours later [vehicle, sCR1 (15 mg/kg), or sCR1sLe$^x$ (15 mg/kg) given as a 200-μl intravenous injection; five animals per group]. For each of the three groups (in order), data showed the following: mean arterial oxygenation of 163 ± 13, 141 ± 12, and 152 ± 11 mm Hg, $P$ = not significant between groups; and serum glucose concentrations were 326 ± 21, 384 ± 44, and 377 ± 6 mg/dl, $P$ = not significant between groups.
17. D. Chiu *et al*., *Stroke* **29**, 18 (1998).
18. L. B. Klickstein, S. F. Barbashov, T. Liu, R. M. Jack, A. Nicholson-Weller, *Immunity* **7**, 345 (1997).
19. S. C. Makrides *et al*., *J. Biol. Chem.* **267**, 24754 (1992).
20. T. F. Choudhri, B. L. Hoh, R. A. Solomon, E. S. Connolly Jr., D. J. Pinsky, *Stroke* **28**, 2296 (1997).


21. We acknowledge the technical assistance of H. Liao and Y. Shan Zou in preparation of tissue for immunohistochemistry, M. Fonseca and G. Palmarini for preparation of murine anti-C1q, and helpful input by T. Choudhri, R. McTaggart, B. Hoh, D. Hoh, and K. Okada. Supported by the Public Health Service (grants R01 HL59488 and R01 HL55397 to D.J.P., and grant R01 NS35144 to A.J.T.). L.J.K. was supported by an American Heart Association and an Alpha Omega Alpha Medical Student Research Award. E.S.C. Jr. participated in this work as part of a Clinical Investigator Development award from the NIH (NS02038), and D.J.P. was supported by a Clinician-Scientist Award from the American Heart Association.

15 March 1999; accepted 21 June 1999


# Correlational Structure of Spontaneous Neuronal Activity in the Developing Lateral Geniculate Nucleus in Vivo


**Michael Weliky*† and Lawrence C. Katz**



**The properties of spontaneous activity in the developing visual pathway beyond the retina are unknown. Multielectrode recordings in the lateral geniculate nucleus (LGN) of awake behaving ferrets, before eye opening, revealed patterns of spontaneous activity that reflect a reshaping of retinal drive within higher visual stages. Significant binocular correlations were present only when cortico-thalamic feedback was intact. In the absence of retinal drive, cortico-thalamic feedback was required to sustain correlated LGN bursting. Activity originating from the contralateral eye drove thalamic activity far more strongly than that originating from the ipsilateral eye. Thus, in vivo patterns of LGN spontaneous activity emerge from interactions between retina, thalamus, and cortex.**


Although visual experience affects visual cortical plasticity during specific critical periods of postnatal development (*1*), many aspects of visual cortical functional organization emerge before visual experience (*2–4*). Thus, visual experience is not required for the initial development of cortical functional organization but is necessary for its maintenance and stability.

Before the onset of visual experience, spontaneous activity within the visual pathway has been proposed to provide instructive cues for guiding orientation and ocular dominance column formation within visual cortex. Correlated patterns of spontaneous activity have been observed in the developing retina (*5*, *6*); however, very little is known about the in vivo patterns of spontaneous activity within higher stages of the visual pathway such as the lateral geniculate nucleus (LGN). It is unlikely that the LGN simply relays patterns of retinal spontaneous activity to the cortex; rather, it reshapes and transforms these patterns. Mechanisms that could underlie these transformations include non-retinal sources of input such as cholinergic brainstem afferents (*7*), massive feedback projections from layer 6 of primary visual cortex (*8*), and LGN and perigeniculate nucleus (PGN) circuitry, which generates endogenous synchronized network oscillations in vitro (*9*, *10*). The eventual patterns of spontaneous activity that underlie the development of visual cortical functional architecture may be quite different from those predicted by retinal activity alone. To investigate


Howard Hughes Medical Institute and Department of Neurobiology, Duke University Medical Center, Durham, NC 27710, USA.

*Present address: Department of Brain and Cognitive Sciences, Meliora Hall, University of Rochester, Rochester, NY 14627, USA.

†To whom correspondence should be addressed. E-mail: weliky@cvs.rochester.edu